Int. J. Electrochem. Sci., 7 **(2012)** 10154 - 10163

International Journal of
ELECTROCHEMICAL
SCIENCE
www.electrochemsci.org

Electropolymerization of *ortho*-Phenylenediamine and its Use for Detection on Hydrogen Peroxide and Ascorbic Acid by Electrochemical Impedance Spectroscopy

Aziah A. Ariffin[1], *Robert D. O'Neill*[2], *M. Z. A. Yahya*[3], *and Zainiharyati M. Zain*[1,*]

[1] Faculty of Applied Sciences, Universiti Teknologi MARA, 40450 Shah Alam, Selangor, Malaysia
[2] UCD School of Chemistry and Chemical Biology, University College Dublin, Belfield, Dublin 4, Ireland
[3] Faculty of Science and Defence Technology, National Defence University of Malaysia, Kem Sungai Besi, 57000 Kuala Lumpur, Malaysia
[*]E-mail: zainihar@salam.uitm.edu.my,

Received: 30 July 2012 / *Accepted:* 8 September 2012 / *Published:* 1 October 2012

Poly(*ortho*-Phenylenediamine) was deposited as a thin film by electrochemical impedance spectroscopy (EIS) and compared to cyclic voltammetry (CV) on Teflon insulated Platinum–Iridium (Pt) disk microelectrode (125 µm diameter) in 300 mM phosphate buffer solution (pH 7.2). This study focuses on the electropolymerization process and electrical properties of P*o*PD-modified microelectrodes, using EIS technique. The estimated thickness of the P*o*PD film was 31 nm with conductivity of 1.1 x 10^{-5} Scm^{-1}. The initial impedance plot shows a semicircle which characterized the charge-transfer resistance at the microelectrode/polymer interface at higher frequency and a diffusion process at lower frequency. Impedance data were fitted to the Randles and a modified Randles circuit models with $\chi^2 = 0.12$ and $\chi^2 = 0.06$ respectively. The capacitive behavior (phase angle = 83°) of the bare Pt microelectrode was transformed to a resistive behavior (phase angle = 13°) after the formation of PoPD layer at lower frequency. The modified electrode was applied as an analytical probe to detect of hydrogen peroxide (H_2O_2) and ascorbic acid (AA). The EIS technique also revealed that the P*o*PD layer blocked the AA species, reflected in the higher impedance observed compared to H_2O_2.

Keywords: Electropolymerization; Poly(*ortho*-Phenylenediamine); Electrochemical impedance spectroscopy; Hydrogen peroxide; Ascorbic acid

1. INTRODUCTION

Poly(*ortho*-Phenylenediamine) (P*o*PD) has been widely developed by several researchers for numerous technological applications, such as protective coating for metals, biosensors, and electrical

and electronic devices [1-3]. The P*o*PD monomer can be easily dissolved in various solvents, making it a good candidate for electropolymerization and the production of thin self-sealing insulating polymer on many electrode surfaces, such as platinum, gold, indium tin oxide (ITO), and copper [4-7]. Several authors [8-14] have reported the electropolymerization and characterization of conducting polymers, namely P*o*PD, polyaniline, polythiophene, and polypyrrole. P*o*PD electropolymerization uses common electrodeposition technique, *e.g.* cyclic voltammetry (CV), characterized by electrochemical impedance spectroscopy (EIS), electrochemical quartz crystal microbalance, Fourier transform infrared spectroscopy, and Raman spectroscopy [6, 15-18]. EIS is a technique which infers more information on the electrochemical interfacial properties of surface-modified electrodes by providing electrical parameters, such as capacitance double layer (C_{dl}), Warburg impedance (infinite diffusion, W), transfer resistance (R_{ct}), solution resistance (R_s), and diffusion coefficient [12, 19].

Martinusz [20] has been reported the influence of applied potential on the modification of Pt and Au macroelectrodes with PoPD has affected the charge transfer and diffusion coefficient. Other reports [18, 21-23] used porous models to explain the modification of P*o*PD film electrodes. These studies suggested that the polymer film is made up of short-band long polymer chains that form into bundles in such a way that only a small part of the metal substrate is covered by the polymeric material [24]. Dai et al. [27] revealed that poly(meta-Phenylenediamine) film on Palladium electrode very permeable to hydrogen peroxide but low permeability for ascorbic acid, uric acid, acetaminophen and cysteine. The permselective property of P*o*PD is increased by electrosynthesized in the absence of added background electrolyte by amperometric calibration [26]. Generally, interference species are determined by amperometry combined with CV [27-29]. However, the amperometry technique has its inherent limitations, such as relatively low output current density, noisy response, and gradual deterioration of enzyme activity, which mainly originates from overvoltage applied to the biosensor [29]. EIS has been introduced as an alternative approach to determine interference species as reported by Shervedani et al. [28]. This technique provided a single experiment, easy to handle with modern computer - controlled instrumentation and also give accessed to the differences between sensing electrode surface in a way not possible by voltammetric techniques due to the wide range of timescales probed by EIS [30]. In this paper, the EIS analysis of the P*o*PD electropolymerization process on the Pt microelectrode with the application of different electrode potential is discussed. These electrochemical parameters obtained were evaluated by a newly proposed modified Randles circuit model [R(RQ)([RW]Q)]. The modified microelectrode is used to detect H_2O_2 and AA using EIS as well.

2. EXPERIMENTAL

2.1 Materials

Ortho-phenylenediamine (*o*-PD), hydrochloric acid (HCl) 37%, and phosphate monobasic (Na_2HPO_4) were purchased from Sigma Aldrich (Germany). Sodium hydroxide (NaOH) was purchased from Merck (Germany). All chemicals were used as received. Teflon-coated platinum-iridium (Pt–Ir) with 125 μm internal diameter from Advent Research Materials (Oxford, UK) was used as a working electrode throughout this study.

2.2 Preparation of Pt Microelectrode

The 2.5 m wire reel with 125 μm internal diameter was reduced by 4 cm. Approximately 1 cm of the Teflon coating at the end of the electrode was removed using a sharp scalpel blade. The end was soldered into a gold clip to connect the working electrode to the circuit. Disk electrodes were prepared by cutting the other end transversely to minimize Teflon distortion and to produce a smooth Pt disk surface [24, 45].

2.3 Electropolymerization and Instrument

P*o*PD electropolymerization was conducted in PBS (pH 7.2) solution containing 300 mM of *o*-PD. A standard electrochemical cell (three electrodes) was used, Pt rod as counter electrode and Ag/AgCl as reference electrode. CV was performed on the polymers with an Autolab PG STAT302 potentiostat/galvanostat (Eco Chemie, Netherlands) controlled by Nova 1.7 electrochemical software (Metrohm, Netherlands) at scan rate of 100 mVs^{-1}. Impedance measurements were performed by varying the voltage with perturbation amplitude of 10 mV rms over a frequency range of 0.01 Hz to 100 kHz using Autolab PG STAT302 (software; Nova 1.7).

3. RESULTS AND DISCUSSION

3.1 Influence of Applied Potential on Impedance Response

The EIS spectrum of bare Pt microelectrode in PBS without *o*-PD monomer (Figure 1) clearly indicates different electrical properties of the P*o*PD layer on the Pt microelectrode (Figure 2d). The impedance of P*o*PD-coated microelectrode is lower (1.3×10^2 kΩ) than that of bare Pt (2.5×10^4 kΩ) due to the effective surface coverage of P*o*PD [31]. Ideal capacitance behavior appears on the Bode plot, which is attributed to a 90° shift and high impedance values at a lower frequency [31]. Thus, uncoated Pt microelectrode exhibited an almost pure capacitance, as shown in the 91° phase shift of the Bode plot (Figure 1b) and a nearly straight line on the Nyquist plot. By contrast, P*o*PD-modified Pt behaved as a non-ideal capacitance because a 90° shift phase and a slanted line on the Nyquist plot were not observed.

CV (Figure 2a) corresponds to potentials at which impedance simulations were performed in the redox reaction potential range from +0.1 V to +0.80 V. The oxidation region was potentially dependent, as presented in the impedance spectrum (Figures 2b to 2e). These findings are in agreement with the report of Martinusz et al. [22]. Figure 2b shows that lower potential (E = +0.1 V) initiates P*o*PD layer formation, where impedance response provides a high-frequency capacitive loop coupled with a low-frequency inductive loop.

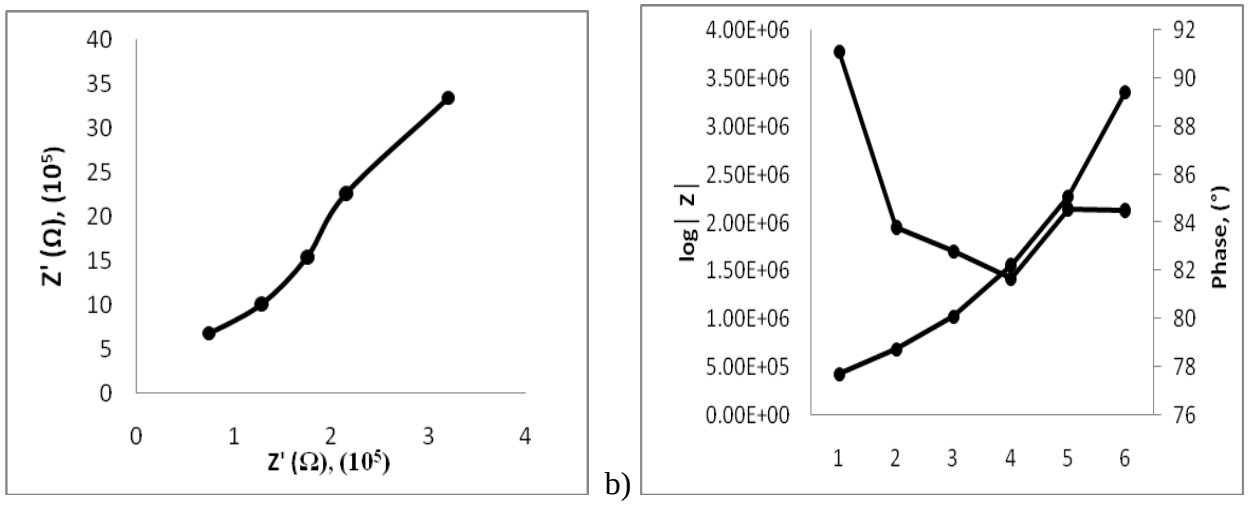

Figure 1. a) Nyquist Plot and b) Bode Plot of uncoated bare Pt in PBS pH 7.2 at +0.5 V, with a frequency range 0.01 Hz to 10^2 kHz.

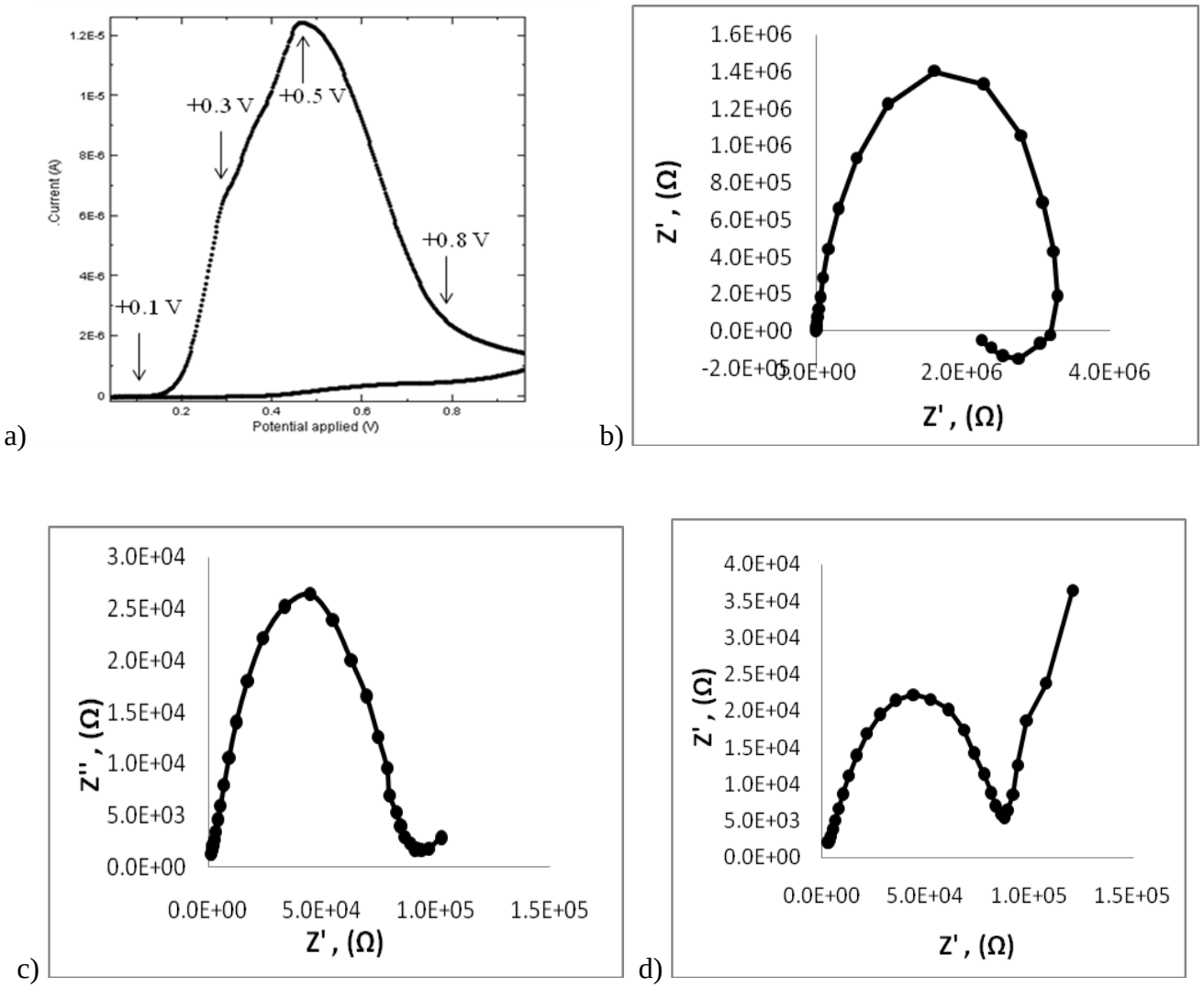

e) 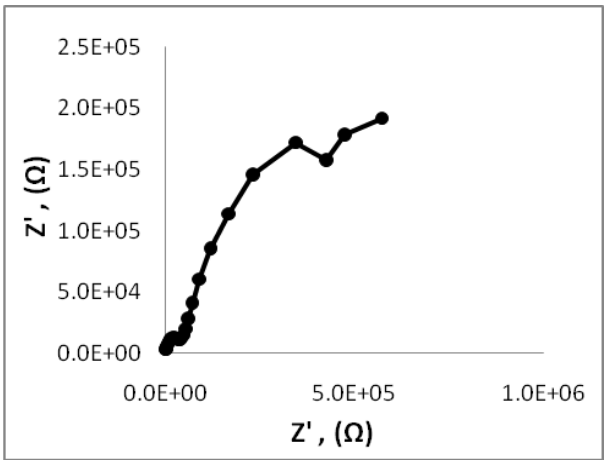

Figure 2. a) CV of P*o*PD electropolymerization and the Nyquist plot of P*o*PD-coated electrode at different potentials; b) +0.1V, c) +0.3V, d) +0.5V, and e) +0.8V, with a frequency range 0.01 Hz to 10^2 kHz.

PoPD was found to be in contrast to Polyaniline (PANi) electropolymerized on Pt foil (2 cm^2) in HCl electrolyte [33] where the inductive behavior at higher potential can reach up to +0.9 V. Figure 2b shows that the inductive loop increased in the imaginary part and decreased in the real part where the impedance move towards the negative part. The existence of inductance behavior on the spectra suggests an adsorption process on the Pt microelectrode surface. Schrebler et al. reported that the impedance data obtained at different applied potentials cannot be fitted using single equivalent circuit such as the Randles circuit model (R(Q[RW]) [34]. Thus, the inductor element (L) is proposed into the circuit because of the inductance influence in the electrochemical system [30, 31] and there are no reports on this process thus far. CV in Figure 2a shows that an obvious change on impedance response with +0.3 V electrode potential (Figure 2c), which was represented by P*o*PD growth onto the Pt microelectrode surface, took place during the measurements. The inductance loop disappeared and was replaced with a short spike that emerged at the lower frequency. A smaller semicircle at a higher to intermediate frequency was observed.

The semicircle represented a charge transfer and capacitance double layer (C_{dl}) phenomena that occurred during initial P*o*PD formation and the short spike suggested that the diffusion-limited process started to occur at the metal-solution interface, but turned to a long spike across lower frequency as the potential increased to +0.5 V (Figure 2d). This diffusion-limited process or W corresponds observed by the increment of current density on voltammogram. On the contrary, at much higher electrode potential, +0.8 V (Figure 2e) resulted in a very small semicircle at higher frequency. The impedance at intermediate frequencies exhibited pronounced capacitive behavior, which can be attributed to the restricted access monomer coating on the electrode surface [5] resulting from the formation of insulating P*o*PD, as evidenced on CV. A P*o*PD film thickness, 31 nm was calculated using equation 1 which agrees with other reports [24, 43] where, d is the film thickness, q_{cv} is the voltammetric charge and A is the electrode area (1.23 x 10^{-4} cm^2).

$$d = \frac{q_{cv}}{A} \qquad [1]$$

The thickness is typically in the range of 10 nm to 35 nm. P*o*PD conductivity using equation 2, where, σ is the conductivity, d is the film thickness, A is the electrode area (1.23 x 10^{-4} cm^2) and R_b is the bulk resistance. It was calculated at 1.1 x 10^{-5} Scm^{-1}, which was slightly lower than the result reported by Oyama et al. [35]. Thus, variation of impedance responses towards different applied potential indicates different electrochemical and electrical properties of the P*o*PD oxidation process.

$$\sigma = \frac{d}{AR_b} \qquad [2]$$

3.2 Equivalent Circuit Model

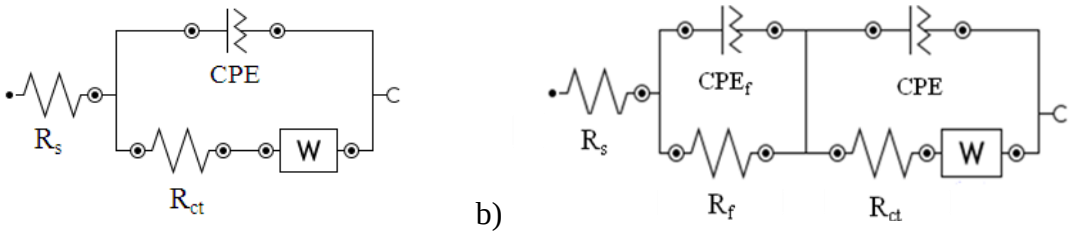

Figure 3. a) ([R(Q[RW])]) and b) [R(RQ)([RW]Q)]. The equivalent circuit is made up of constant phase element (CPE), film constant phase element (CPE_f), R_s, W, R_{ct}, and film resistance (R_f).

Nova 1.7 EIS analysis software was used to interpret and evaluate the impedance data. The equivalent circuit model comprises an interface capacitance (C_{dl}), R_{ct}, R_s and other elements can been fitted to the experimental results. Theoretical equations have been used to calculate the interface elements in the circuit and give in results that correspond well with the fitted parameter values, thereby confirming the validity of the equations [36]. (R(Q[RW]) (Figure 3a) is commonly used to gain information on the investigated active systems derived from experimental data for electrical parametric identification. Several complex circuits were extensively studied, and a fitting program eases the impedance interpretation to facilitate the modeling of electrolyte – electrode interface coated with organic and conducting films [8, 37-38].

Martinuzs et al. [20] did not employ the (R(Q[RW]), but proposed other complex circuits because the results they predicted were purely capacitive behavior at a lower frequency and were not applicable to (R(Q[RW]). By contrast, Lang et al. [40] developed a complex brush model to show that showed the gold surface is not fully covered with P*o*PD due to the surface roughness and also give longer and shorter polymer chains. However, this study proposed the (R(Q[RW]) and the [R(RQ)([RW]Q)] to initiate a better understanding of the electrochemical process and properties of P*o*PD during electropolymerization. The impedance spectra were fitted to the Randles equivalent circuit, which was made up of a parallel combination of a constant phase element (CPE), charge transfer resistance (R_{ct}), W impedence, and solution resistance (R_s). The perfect semicircle was hardly

achieved in this real system [41], thus, a CPE was used instead of a double-layer capacitance (C_{dl}), as shown in Figure 2a.

Figure 3 shows the EIS parameters of the electrodeposited P*o*PD in PBS pH 7.2, which were obtained by fitted experimental data using both equivalent circuit models. These results indicate that electron transfer was highly promoted in the P*o*PD electropolymerization on the electrode surface at the applied potential of +0.5 V. In addition, the fitness of P*o*PD in PBS pH 7.2 was reasonable with both models because [R(RQ)([RW]Q)] (χ^2 = 0.12) was the most fitted model compared with (R(Q[RW]) (χ^2 = 0.06). Vyas et al. investigated the ionic conductivity of multi-layer poly (*p*-phenylene vinylene) [42] using [R(RQ)([RW]Q)] by adding the R_f and CPE_f elements. Our results are aligned with the findings of Tonosaki et al. [43], which also applied modified Randles to evaluate the P*o*PD/Poly (vinyl alcohol) composite film. However, this study proposed a different combination of R_f and CPE_f, where these parameters may represent a self-assembled polymer monolayer [44], as illustrated in Figure 2b. After fitting the diffusion coefficient, (D) can be determined using the following equation [31, 42]:

$$\sigma = \frac{RT}{n^2 F^2 A}\left(\frac{1}{D_{ox}^{1/2} C_{ox}} + \frac{1}{D_{red}^{1/2} C_{red}}\right) \quad [3]$$

where *n* is the number of transferred electrons, *R* is the gas constant (8.314 $J \cdot mol^{-1} \cdot K^{-1}$), F is the Faraday constant (96485 $C \cdot mol^{-1}$), T is room temperature (298 K), A is the electrode area (1.23 x 10^{-4} cm^2) and σ is Warburg parameter obtained after fitting. Assuming diffusion coefficients $D_{ox} = D_{red} = D$ and concentrations $c_{ox} = c_{red} = c_{bulk}$, as expressed in Equation 4, all the fitting parameters and calculated diffusion coefficients are tabulated in Table 1.

$$D = \left(\frac{\sqrt{2}RT}{n^2 F^2 A \sigma c_{bulk}}\right)^2 \quad [4]$$

Table 1. EIS parameters of electrodeposited PPD on Pt microelectrode obtained by experimental fitting data to the equivalent circuit model in Figure 2.

Circuit	Rs, kΩ	Rct, kΩ	R_f, kΩ	CPE_f, μFcm^{-2}	CPE, μFcm^{-2}	D, $\Omega.s^{-1/2}$	χ^2
[R(Q[RW])]	1.95	84.59	-	-	0.15	16.82 x 10^5	0.12
[R(RQ)([RW]Q)]	1.06	81.37	1.55	2.23 x 10^{-4}	0.11	11.57 x 10^5	0.06

3.3 Detection of Hydrogen Peroxide and Ascorbic Acid

The permeability of H_2O_2 (the signal transduction molecule for several oxidase-based biosensors/the biosensor enzyme signal molecule) and AA (archetypal interference compound) [25] at the P*o*PD-modified Pt microelectrode was conducted using amperometry and CV techniques [24, 45]. Results indicated that P*o*PD showed excellent permeability to H_2O_2 and minimized interference

problems by blocking AA and other interference species, such as dopamine and uric acid [28]. To the best of our knowledge, this study was the first to report the interference compound of AA detected using EIS.

Figure 4c shows that the AA concentration trend has higher impedance (4.4 kΩ to 6.4 kΩ) compared with H_2O_2 (2.8 kΩ to 3.7 kΩ) because the larger size of AA molecules cannot pass through to the P*o*PD layer [46] compared with the small H_2O_2 molecules. A straight line (Figure 3a) was observed at various H_2O_2 concentrations in the range of 0.01 M to 0.1 M, where the electrode was influenced by capacitive behavior (phase angle: 60° to 65°), which is dominant at higher frequencies because of the electron transfer kinetic of redox species at the electrode surface. Less than 1 kHz of the modified electrode behaved as a resistor as the decrease of phase angle nears 0°. Figure 4b indicates that the charge transfer resistance was inversely proportional to H_2O_2 concentration. In other words, the R_{ct} values decreased upon the addition of H_2O_2 into the PBS solution. This result correlate with that of Shervedani et al. [29] who examined Au-MPA-Gox SAMs electrode as biocatalytic interface. Therefore, P*o*PD/Pt exhibited good impedance response towards H_2O_2 and AA blocking at +0.2 V, and agrees with previous literature.

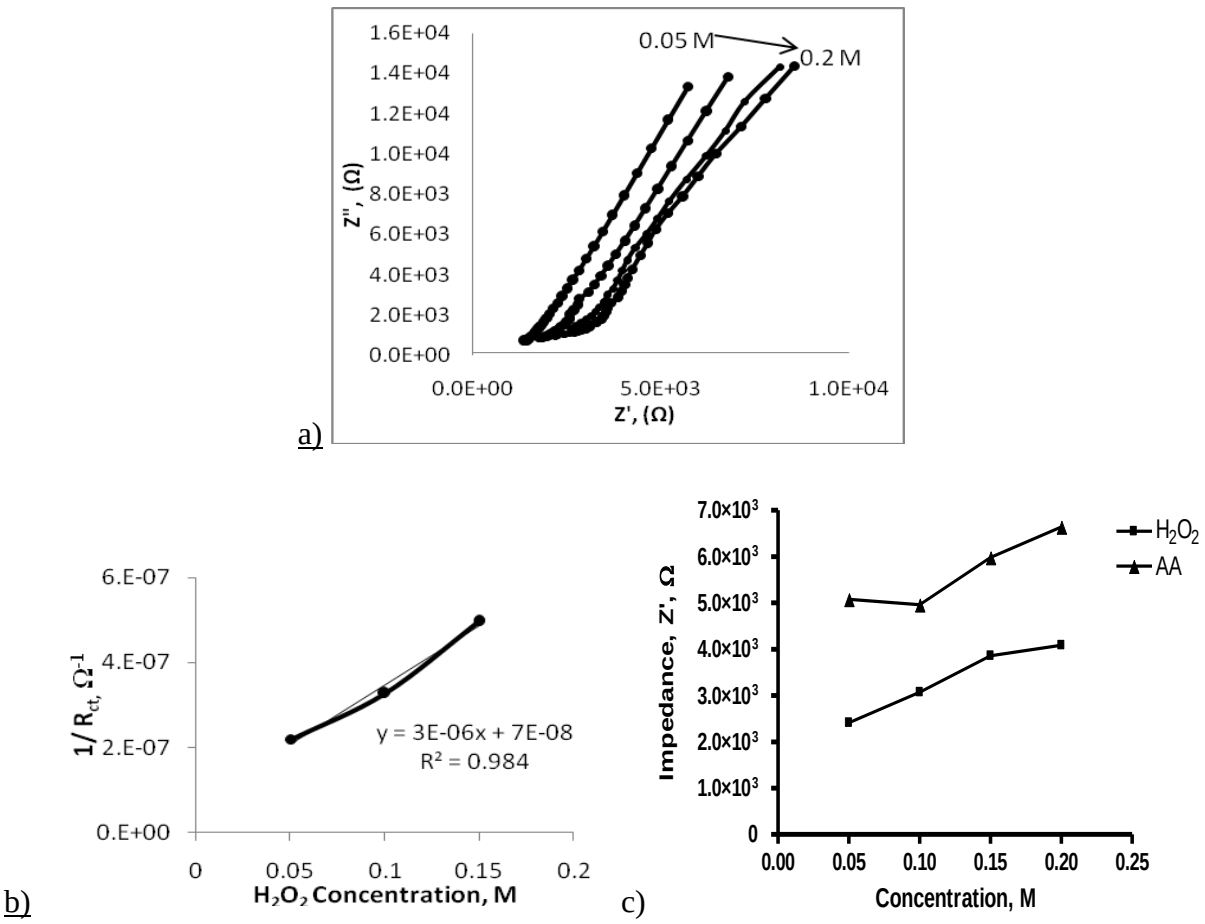

Figure 4. a) Impedance response of H_2O_2 (0.05 M to 0.2 M) in PBS pH 7.2 on P*o*PD/Pt electrode, electrode potential; +0.2 V, a) with a frequency range of 1 kHz to 10^2 kHz, b) Linear plot of 1/Rct vs H_2O_2 concentration, y = 3.0 x 10^{-6}x + 7.0 x 10^{-8}, r^2 = 0.98, c) Impedance versus AA and H_2O_2 concentration.

4. CONCLUSION

Electrochemical characterization of the P*o*PD layer was conducted using CV and EIS techniques. The increment of applied potential at lower frequencies changed the electrode behavior from capacitive (phase shift: 83°) to resistive (phase shift: < 45°) because of the P*o*PD layer formation. The P*o*PD-modified electrode rejected AA molecules by showing the highest impedance (4.4 kΩ to 6.4 kΩ) in contrast to the H_2O_2 species, which showed lower impedance values (2.8 kΩ to 3.7 kΩ).

ACKNOWLEDGMENTS

This work was supported by FRGS Grant (600-RMI/ST/FRGS 5/3/Fst (12/2011). A. A. Ariffin would like to thank the Ministry of Higher Education (MOHE), Malaysia for her MyMaster Scheme Award.

References

1. J.W. Long, C.P. Rhodes, A.L. Young and D.R. Rolison, *Nano Letters*., 3 (2003) : 1156.
2. D. Chirizzi and C. Malitesta, *Sensors and Actuators B: Chemical*., 157 (2011) : 211.
3. S.R. Sivakkumar and R. Saraswathi, *J. Electroanal. Chem.*, 34 (2004) : 1147.
4. G. Camurri, P. Ferrarini, R. Giovanardi, R. Benassi and C. Fontanesi, *J. Electroanal. Chem.*, 585 (2005) : 183.
5. S.M. Sayyah, M.M. El-Deeb, S.M. Kamal and R.E. Azooz, *J. Applied Polymer Sci*., 112 (2009) 3697.
6. E.Y. Pisarevskaya, T.M. Serdyuk, E.V. Ovsyannikova, A.K. Buryak and N.M. Alpatova, *Synthetic Metals.*, 160 (2010) : 2366.
7. V. Branzoi, L. Pilan and F. Branzoi, *Molecular Crystals and Liquid Crystals*., 416 (2004) : 66.
8. A. S. Sarac, M. Ates and, B. Kilic, *Int. J. Electrochem. Sci.* 3 (2008) 778.
9. C. C. Hu and C. H.Chu. *J. Electroanal. Chem*., 503 (2001) 107.
10. L. Niu, Q. Li, F. Wei, X. Chen and H.Wang, *J. Electroanal. Chem*., 544 (2003) 1166.
11. M. Ates, *Int. J. Electrochem. Sci.*, 4 (2009) 1005.
12. M. Ates, *Progress in Organic Coatings*., 71 (2011) 4.
13. S. Komaba and T. Osaka, *J. Electroanal. Chem*., 453 (1998) 21.
14. M. Sharifirad, A. Omrani, A. A. Rostami and M. Khoshroo, *J. Electroanal. Chem*., 645 (2010) 149.
15. G.G. Lang, M. Ujvari, T.A. Rokob and G. Inzelt, *Electrochimica Acta*., 51 (2006) 1680.
16. O. Levin, V. Kondratiev, and V. Malev, *Electrochimica Acta*., 50 (2005) 1574.
17. T. Maiyalagan and B. Viswanathan, *Indian Journal Of Chemistry*,. 48A (2009) 198.
18. A. Malinauskas, M. Bron, and R. Holze, *Synthetic Metals*., 92 (1994) 128.
19. V. Freger and S. Bason, *J. Membrane Sci.*,. 302 (2007) 3.
20. K. Martinusz, G. Lang and G. Inzelt, *J. Electroanal. Chem*., 433 (1997) 1.
21. G. Lang, M. Ujvari and G. Inzelt, *Electrochemica Acta*, 46 (2001) 4162.
22. G. Lang and G. Inzelt, *Electrochemica Acta*., 44 (1999) 2037.
23. G. Lang, M. Ujvari and G. Inzelt, *J. Electroanal. Chem*., 572(2) (2004) 288.
24. S.J. Killoran and R.D. O'Neill, *Electrochimica Acta*, 53 (2008) 7303.
25. S.A. Rothwell, C.P. McMahon and R.D. O'Neill, *Electrochimica Acta*., 55 (2010) 6440.
26. S.A. Rothwell, S.J. Killoran, E. M. Neville, A. M. Crotty and R.D. O'Neill, *Electrochem. Commun.*10 (2008) 1079.
27. Y.Q. Dai, D. Zhou and K. Shiu, *Electrochimica Acta*, 52 (2006) 299.
28. T. Selvaraju and R. Ramaraj, *J. Applied Electrochem.* 33 (2003) 759.

29. R.K. Shervedani, A.H. Mehrjardi, and N. Zamiri, *Bioelectrochemistry.*, 69 (2006) 202.
30. R. Pauliukaite, M. E. Chiga, O. F.Filho and C. M. A. Brett, *Electrochimica Acta.*, 55 (2010) 6239.
31. C.F. Sanchez, C.J. McNeil and K. Rawson, *TrAC Trends in Anal. Chem.*24 (2005) 39.
32. O. Panke, T. Balkenhohl, J. Kafka, D. Schafer and F. Lisdat, *Adv Biochem Engin/Biotechnol*., 109, (2007) 199.
33. W.C. Chen, T.C. Wen, C.C. Hu, A. Gopalan, *Electrochemica Acta.*, 47 (2002) 1312.
34. R. Schrebler, H. Gomez, R. Cordova, L.M. Gassa and J.R. Vilche, *Synthetic Metals*., 93 (1998) 190.
35. N. Oyama and T. Oshaka, *Synthetic Metals*., 18 (1987) 379.
36. W. Franks, I. Schenker, P. Schmutz, and A. Hierlemann, *Electrodes for Biomedical Applications* 52 (2005) 1295.
37. M. E. Orazem and B. Tribollet, *Electrochemical Impedance Spectroscopy*, John Wiley & Sons Inc, New Jersey (2008) 334.
38. M.R. Abidian and D.C. Martin, *Biomaterials.*, 29 (2008) 1278.
39. A. Amirudin and D. Thierry, *Progress in Organic Coatings.*, 26 (1995) 5.
40. G. Lang, M. Ujvari and G. Inzelt, *Electrochemica Acta*, 46 (2001) 4159.
41. J.R. Mcdonald and E. Barsoukov, *Fundamentals of Impedance Spectroscopy*, , John Wiley & Sons Inc, New Jersey, (2005) 80.
42. R.N. Vyas and B. Wang, *Int. J. Mol. Sci.*11 (2010) 1958.
43. T. Tonosaki, T. Oho, K. Isomura and K. Ogura, *J. Electroanal. Chem*.., 520 (2002) 91.
44. R.N. Vyas and B. Wang, *Electrochem. Commun*., 10 (2008) 417.
45. S.A. Rothwell, S.J. Killoran and R.D. O'Neill, *Sensors*., 10 (2010) 6441.
46. R. Mazeikiene and A. Malinauskas, *Synthesis Metals*., 64 (2004) 122.